Recent changes in the snout position and surface velocity of Gangotri glacier observed from space

6 authors, including:

Tajdarul Hassan Syed

Indian Institute of Technology Kanpur

59 PUBLICATIONS   **3,133** CITATIONS

SEE PROFILE

Eric J Fielding

California Institute of Technology

306 PUBLICATIONS   **15,802** CITATIONS

SEE PROFILE

Some of the authors of this publication are also working on these related projects:

Project   Remote sensing of ground deformation for monitoring groundwater management practices: application to the Santa Clara Valley during the 2013-2015 California drought View project
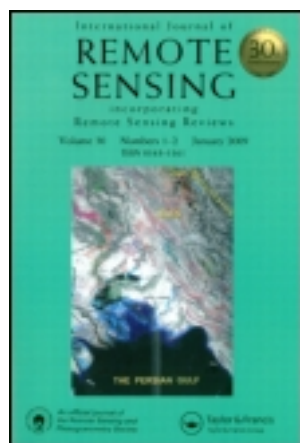
Project   Imaging Fault Slip Before, During, and After Earthquakes View project

Recent changes in the snout position and surface velocity of Gangotri glacier observed from space

Puneet Saraswat[a], Tajdarul H. Syed[b], James S. Famiglietti[cd], Eric J. Fielding[e], Robert Crippen[e] & Nishant Gupta[b]

[a] Department of Applied Geophysics, Indian School of Mines, Dhanbad, India

[b] Department of Applied Geology, Indian School of Mines, Dhanbad, India

[c] Department of Earth System Science, University of California, Irvine, CA, USA

[d] UC Center for Hydrologic Modeling, University of California, Irvine, CA, USA

[e] Jet Propulsion Laboratory, California Institute of Technology, Pasadena, CA, USA

PLEASE SCROLL DOWN FOR ARTICLE

Taylor & Francis
Taylor & Francis Group

Recent changes in the snout position and surface velocity of Gangotri glacier observed from space

Puneet Saraswat[a], Tajdarul H. Syed[b]*, James S. Famiglietti[c,d], Eric J. Fielding[e],
Robert Crippen[e], and Nishant Gupta[b]

*[a]Department of Applied Geophysics, Indian School of Mines, Dhanbad, India; [b]Department of
Applied Geology, Indian School of Mines, Dhanbad, India; [c]Department of Earth System Science,
University of California, Irvine, CA, USA; [d]UC Center for Hydrologic Modeling, University of
California, Irvine, CA, USA; [e]Jet Propulsion Laboratory, California Institute of Technology,
Pasadena, CA, USA*

Glacier mass variations have a direct impact on some of the key components of the
global water cycle, including sea level rise and freshwater availability. Apart from being
one of the largest Himalayan glaciers, Gangotri is one of the sources of water for the
Ganges river, which has a considerable influence on the socioeconomic structure of a
largely over-populated catchment area accounting for ∼26% of India's landmass. In this
study, we present the most recent assessment of the Gangotri glacier dynamics, combin-
ing the use of interferometric techniques on synthetic aperture radar data and sub-pixel
offset tracking on Advanced Spaceborne Thermal Emission and Reflection Radiometer
(ASTER) satellite imagery. Results show that on average, the Gangotri glacier snout
has receded at a rate of 21.3 ± 3 m year^{-1} over a period of 6 years (2004–2010).
While glacier surface velocity near the snout is estimated to be between 24.8 ± 2.3 and
28.9 ± 2.3 m year^{-1}, interior portions of the glacier recorded velocities in the range of
13.9 ± 2.3 to 70.2 ± 2.3 m year^{-1}. Further, the average glacier surface velocity in the
northern (lower) portions (28.1 ± 2.3 m year^{-1}) is observed to be significantly lower
than in the southern (higher) portions (48.1 ± 2.3 m year^{-1}) of the Gangotri glacier.
These values are calculated with an uncertainty of less than 5 m year^{-1}. Results also
highlight a consistent retreat and non-uniform dynamics of the Gangotri glacier.

1. Introduction

The impact of climate change on glaciers of the world has been a topic of active concern
in recent times (Syed et al. 2007; Bagla 2009; Cogley et al. 2010). While glacial melt is a
major source of freshwater that contributes to global mean sea level rise (Meier et al. 2007;
Jacob et al. 2012), decreasing glacial mass has an impact on the freshwater resources of
some of the largest river basins in the world, including that of the Ganges (e.g. Kumar,
Singh, and Sharma 2005; Mall et al. 2006; Immerzeel, van Beek, and Bierkens 2010;
Kaser, Grosshauser, and Marzeion 2010). Fluctuations in the recession rate of glaciers dur-
ing recent years have initiated widespread discussions, especially in the context of global
warming and its effects (Dyurgerov and Meier 2005). Similar ice mass changes have also
been reported in the Garhwal region of the Himalayas (Kulkarni et al. 2005; Bhambri,
Bolch, and Chaujar 2011a, 2011b; Kulkarni et al. 2011; Bolch et al. 2012). However, the

*Corresponding author. Email: tsyed.ismu@gmail.com

status of the Gangotri glacier warrants further investigation, particularly in the context of climate change resulting in continuous retreat, negative mass balance, and early melting of seasonal snow cover (Negi et al. 2012).

Glaciers cover about 40,800 km^2 of the Himalayan and Karakoram mountain region, and are one of the main sources of water to some of the largest rivers in the world, including the Ganges, Brahmaputra, and Indus (Kulkarni et al. 2011; Bajracharya and Shrestha 2011; Bolch et al. 2012). Approximately 10% of the summer discharge of the Ganges is attributed to melt waters from glaciers (Barnett, Adam, and Lettermaier 2005; Jain, Agarwal, and Singh 2007; Immerzeel, van Beek, and Bierkens 2010; Bolch et al. 2012). Rapid depletion of glaciers has had adverse effects on the flow regime of major Himalayan rivers, and can even lead to catastrophic events such as glacial lake outbursts (Govindha 2010; Shrestha, Eriksson, and Mool 2010; Ashraf, Naz, and Roohi 2012) and consequent flooding in the upper reaches of these rivers, affecting the lives of millions of people residing in the Indo-Gangetic plains (Richardson and Reynolds 2000; Bolch et al. 2012).

In spite of their hydrologic, climatic, and socioeconomic significance, opportunities for precise and continuous monitoring of the Himalayan glaciers are limited by logistical and terrain-induced difficulties. Observations of Earth's surface using satellite data have proven to be very useful in such monitoring; recent developments in high-resolution image acquisition have facilitated more precise monitoring of glacier movement (Luckman, Quincey, and Bevan 2007; Kumar, Venkataraman, and Hogda 2011; Kumar et al. 2011). Further, satellite data enables a gross analysis of glacier mass budgets, overcoming some of the problems of accessibility and sustainability of long-term measurements, that can later be verified with ground-based surveys (Kumar et al. 2008). The potential of remote sensing for glacier mass balance and velocity mapping has been demonstrated with optical (e.g. Kääb 2005; Scherler, Leprince, and Strecker 2008), synthetic aperture radar (SAR) (e.g. Luckman, Quincey, and Bevan 2007), and thermal infrared sensors (e.g. Nakawo, Yabuki, and Sakai 1999), and elevation models (Bolch, Pieczonka, and Benn 2011), among others. Developments in deriving flow rates and monitoring Himalayan glacier retreat using optical images have been made by Kääb (2005). However, this approach is sometimes limited by weather, clouds, and shadows in areas of high relief.

In a novel approach, the current study presents one of the most comprehensive assessments of the Gangotri glacier in recent times (2004–2011). The methodology entails the utilization of interferometric SAR (InSAR) coherence and sub-pixel offset tracking. While complementing most previous studies, the result presented here establishes the effectiveness of the techniques implemented to produce robust estimates of areal changes and glacier surface velocity in near real time. But, perhaps most importantly, this is one of the few studies which has shown the melting trend of Gangotri glacier over a considerably continuous period during recent times (2004–2011).

2.   Study area

The Gangotri glacier is a valley-type glacier and one of the largest Himalayan glaciers located in Uttarkashi district of Uttarakhand, India (Figure 1). Extending between the latitudes 30° 43′ 22″ N–30° 55′ 49″ N and longitudes 79° 4′ 41″ E–79° 16′ 34″ E, Gangotri is the only major Himalayan glacier that flows towards the northwest. It spans a length of 30.2 km, its width varies between 0.20 and 2.35 km, and it thereby covers an area of about 86.32 km^2. While the average thickness of the Gangotri glacier is ∼200 m, its surface elevation varies from 4000 to 7000 m above mean sea level (Jain 2008). Gangotri has three main tributaries, namely the Raktvarna, the Chaturangi, and the Kirti, with lengths
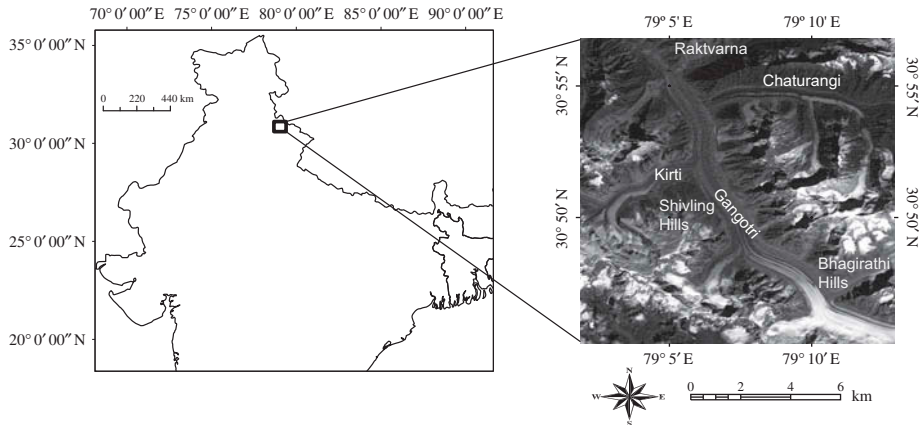
Figure 1. Location of the Gangotri glacier in the overall Indian perspective. Also shown is a magnified view of the study area using an ASTER image illustrating the locations of the Gangotri glacier and its tributaries (Kirti, Raktvarna, and Chaturangi). The figure also marks the locations of the Shivling and Bhagirathi hills.

of 15.90, 22.45, and 11.05 km, respectively (Figure 1). Additionally, there are more than 18 small tributary glaciers of Gangotri and its tributaries. Gangotri and other glaciers in this region are mostly fed by the summer monsoon and partly by winter snow. Western disturbances cause heavy snowfall from December to March over this region (Thayyen and Gergan 2010). Generally, seasonal melting starts in the month of May and continues till October (Dobhal, Gergan, and Thayyen 2008).

3. Data and methods

3.1. Coherence detection for glacier retreat

InSAR provides avenues to study glaciers in terms of snout and glacial lake monitoring, as well as ground displacement and topographic variations, using interferograms (Luckman, Quincey, and Bevan 2007; Kumar et al. 2008; Capps et al. 2010). Glacier monitoring using InSAR is advancing towards new frontiers; in this study, we develop coherence maps using SAR image pairs to map the location of the snout of the Gangotri glacier. Previously, this technique has been utilized to delineate glacier extent (Atwood, Meyer, and Arendt 2010) and to identify debris-covered portions of glaciers in the northwest Himalayas (Frey, Paul, and Strozzi 2012). In this study, we utilize the coherency attribute between two SAR images for snout monitoring. We estimate coherence of interferograms made from two SAR acquisitions with the spatial correlation of the InSAR phase over small areas of pixels (Fielding et al. 2005). This phase correlation is related to the relative displacement of the scattering objects within each pixel and large surface motion during the time between two SAR acquisitions. While higher values of coherence are associated with small motion and disruption of the surface, lower values are representative of considerable displacement or surface changes over a specified time period. Practically, it can help in understanding the stability of the terrain imaged. Ice, which is constantly melting and accumulating in addition to flowing laterally, shows very low relative coherence even if the images have a small temporal baseline. InSAR coherence estimates typically involve a bias of ~20% in areas

of low coherence, so we consider relative values of coherence instead of the absolute values in order to characterize the stability of the surface. The terminus, where the ground is exposed as a consequence of glacier retreat, shows better coherence compared to the pixels within the glacier (Atwood, Meyer, and Arendt 2010). To delineate a high coherence zone, which is ice-free ground, we apply a threshold of 0.4 (40%) to InSAR correlation to select the areas of high coherence from the interferograms. This is based on the assumption that high coherence values are largely due to the presence of ice-free surface near the glacier snout. The retreat rate is calculated as the distance measured between the mapped snout in first image pair (in this case 2004–2005) and last image pair (2009–2010) along the central flow line of the glacier. However, coherence of the non-glaciated portions of land ahead of the terminus may be subsequently affected by flowing melt water from the glacier. This shortcoming was surpassed by selecting images during early summer (March–May) and early winter (October–December) with relatively short acquisition intervals over the Gangotri region. The coherence analysis is based on InSAR, incorporating data sets acquired by the advanced synthetic aperture radar (ASAR) instrument mounted on the Envisat satellite (Image Mode; see Table 1). The orbital models for Envisat used in this study were obtained from ESA Doris orbits (DOR) and processing was performed with the JPL/Caltech ROI_pac software (Rosen et al. 2004). Digital elevation model (DEM) data are required to remove and model topographic phase contributions, and to orthorectify the data for intercomparison. Here, we use NASA's Shuttle Radar Topographic Mission (SRTM) (Rodriguez, Morris, and Belz 2006) DEM with voids filled by other sources, available from Consultative Group on International Agricultural Research (CGIAR) Consortium for Spatial Information (CGIAR-CSI) (http://srtm.csi.cgiar.org/). These void-filled DEMs (SRTM CGIAR version 3) are particularly effective for the study area since they are constructed using topographic maps and information from local topography.

However, at times InSAR fails to produce reliable measurements of ice motion for fast moving glaciers primarily due to temporal decorrelation or loss of coherence, in the absence of optimal temporal baseline between the image pairs. This aspect is one of the major limitations associated with this technique. Further, steep slopes, particularly in the Gangotri region, inhibit an across-track view of the glacier and render SAR data from the widely available satellites unreliable for glacier velocity measurements. Due to the absence of Envisat SAR pairs with short time intervals over the study area (minimum possible

Table 1. List of the Envisat ASAR images used as pairs for the computation of coherence maps.

Image acquisition date	Pairs	Track	Orbit
30 October 2004	Pair 1	00370	13591
19 March 2005		00370	15955
13 October 2004	Pair 2	00012	11088
5 October 2004		00012	13593
8 May 2007	Pair 3	00012	27120
27 April 2010		00012	42651
5 October 2004	Pair 4	00012	13593
27 April 2010		00012	42651
25 October 2005	Pair 5	00012	19104
8 May 2007		00012	27120
12 May 2009	Pair 6	00012	37641
27 April 2010		00012	42651

repeat time of Envisat was 35 days, but not every orbit had SAR images acquired), temporal decorrelation is a major issue encountered in this study. For the available pairs, the glacier motion is large enough to cause incoherent InSAR leading to temporal decorrelation. Hence, the absence of good coherence between subsequent SAR image pairs makes it difficult to measure the Gangotri ice velocity with Envisat InSAR.

3.2. *Velocity measurements using pixel offset tracking*

Mapping the glacier surface velocity is crucial for characterizing ice dynamics and quantifying glacier ice mass balance (Bindschadler and Scambos 1991; Joughin et al. 2002; Rignot and Thomas 2002). In order to overcome the previously mentioned region-specific limitation of InSAR in mapping glacier velocity, we took an alternative approach to monitor glacier velocities utilizing sub-pixel offset tracking on nadir-viewing near infrared (NIR) imagery from the Advanced Spaceborne Thermal Emission and Reflection Radiometer (ASTER). This technique utilizes cross-correlation between two images to estimate surface velocities, details of which are illustrated in Scherler, Leprince, and Strecker (2008). Pixel offset tracking or sub-pixel correlation is a technique to measure the motion of spatially coherent features through time between two images (Crippen 1992). In glaciology, these features generally consist of crevasses, undulations, and moraines (Konig, Winther, and Isaksson 2001). The horizontal displacement thus obtained can be used to generate velocity maps utilizing the time difference between the images pairs. In this study, the ENVI- and IDL-based processing software, Co-registration of Optically Sensed Images and Correlation (COSI-Corr) (Leprince et al. 2007), is used for the said purpose. This method has been successfully used for measuring glacier velocities such as those in Stearns, Hamilton, and Reeh (2005), Howat et al. (2008), Scherler, Leprince, and Strecker (2008), Debella-Gilo and Kääb (2011), Herman, Anderson, and Leprince (2011), and Willis et al. (2012). Initially, a DEM is used to generate approximate tie points for the master image, and we used the same SRTM 3-arcsecond DEM with the voids filled by the CGIAR group (Version 3) as described above. Tie points are then subjected to an optimization algorithm in order to generate precise ground control points to orthorectify the master image. Once the master image is orthorectified, ensuing slave images are orthorectified using the same master image. After successful orthorectification and co-registration of image pairs, a correlation algorithm is then applied by moving the correlation windows across the prepared images on a regular grid. Distinctive features are tracked between image pairs and their displacement is calculated to produce displacement maps and their corresponding signal-to-noise ratio (SNR) maps. Note that the methodology implemented here is exactly the same as that presented in Scherler, Leprince, and Strecker (2008) and is most appropriate for additional details on the methodology and functionality of COSI-Corr.

In order to overcome the limitation of producing high quality velocity estimates from InSAR, a sub-pixel correlation or offset tracking technique is employed on ASTER L1A satellite imagery acquired for the region. Table 2 enlists the details of the ASTER L1A data set analysed in this study. For better results, maximum care is taken to obtain images with less snowfall and cloud cover, especially over the Gangotri glacier. In order to analyse the motion over the entire length of the glacier, we acquired ASTER L1A data for two frames covering the lower and upper reaches of the Gangotri glacier. Both frames were acquired on the same date and with the same acquisition parameters but processed separately. Another associated advantage of ASTER imagery over SAR imagery for such difficult terrain is the

Table 2.   Details of ASTER images used in the study.

Image ID	Acquisition date	Incidence angle (NIR)	Pairs
Imagery covering lower reaches of the Gangotri glacier			
AST_L1A_003_08192005053458_08222005102857	19 August 2005	5.729	Pair 1
AST_L1A_003_10092006053458_10122006133732	9 October 2006	5.729	
AST_L1A_00310102009052928_20120215162647_ 25802	10 October 2009	−5.732	Pair 2
AST_L1A_00310292010052905_20120215162647_ 25798	29 October 2010	−5.735	
AST_L1A_00310162011052901_20120215162647_ 25804	16 October 2011	−5.727	Pair 3
Imagery covering upper reaches of the Gangotri glacier			
AST_L1A_00310102009052937_20120322162403_ 27825	10 October 2009	−5.732	Pair 4
AST_L1A_00310292010052914_20120322162403_ 27819	29 October 2010	−5.735	
AST_L1A_00310162011052910_20120322162403_ 27816	16 October 2011	−5.727	Pair 5

availability of the 3N (NIR) band with nadir-viewing geometry and 15 m spatial resolution, thus minimizing topography-induced errors in the velocity estimates. The images used in this study are mostly acquired during the month of October, which is the end of the melting season.

3.3.   *Uncertainty analysis*

A number of factors contribute to uncertainties in the coherence-based estimates of glacier retreat rate, including DEM, orbital, and baseline errors. Errors in velocity estimates obtained using pixel offset tracking can again be attributed primarily to DEM errors, which are transferred in the form of orthorectification errors to the orthorectified master image. The SRTM 3-arcsecond DEM that we used has voids filled by the CGIAR group (Version 3), so the DEM quality is variable. The voids in SRTM version 2 are extensive in the steep slopes of the Himalayas. We chose ASTER pairs with the same look angle to minimize the effects of DEM errors since both images have the same viewing geometry. Kääb (2002) discussed these anomalies as a ground position error, which is about 3 m for moderately inclined terrains.

Additionally, uncertainties from resampling and image cross-correlation processes are generally much smaller than the pixel size of 15 m; hence, matches with uncertainties greater than one pixel are usually discarded during the processing (Scherler, Leprince, and Strecker 2008). The cumulative error in velocity estimates is less than 5 m year^{-1} for the data sets used in this study. This error is estimated by computing surface velocity for locations where stable ground is exposed typically near the snout to keep other influencing factors such as slope and surface conditions as close to the glacier as possible. Since surface velocity should be ideally zero in these locations, any value other than zero is approximated as the error. In order to quantify the error, we concentrated on velocities estimated for an area in front of the snout (Figure 4(*a*) (Box 1)), which is observed to be ice-free in all of the images used in this study. Analysis showed that velocities estimated in this study suffer

from a possible bias (mean) of about 4.2 m year^{-1} and an error (standard deviation) of about 2.3 m year^{-1}. The high precision in the observed estimates can be attributed to several factors such as (1) low cloud cover in the ASTER images, (2) the scenes are obtained for the same time period (late summer and fall), which helped to eliminate errors related to snowfall and changes in solar illumination, and (3) the time span between paired ASTER images are mostly kept at nearly 1 year, which provides a resolvable time window to derive glacier surface velocities.

4. Results

4.1. Glacier recession from 2004–2010

Shown in Figures 2(*a*) and (*b*) are the InSAR coherence maps of the Gangotri glacier region obtained from image pairs with the shortest possible acquisition intervals in order to locate the snout of the glacier with improved accuracy. The detail of interferometric pairs chosen to study short and long-term variations of the Gangotri glacier is shown in Table 1. For the reasons stated above we present results from coherence mapping for Pair 1 (Figure 2(*a*)) and Pair 6 (Figure 2(*b*)). Thus, it can be observed in Figures 2(*a*) and (*b*) that by stretching the values in the coherence maps, the majority of the region registered low coherence, caused mainly due to accumulation and ablation of snow and ice and also due to steep slopes. However, regions near the northern flank of the glacier show high coherence (>40%), which is attributed to the fact that the snout of the glacier has retreated, exposing boulders and moraines. Hence, these are the areas which show more relative stability over a considerable period of time (typically a few months). Areas further down the valley are likewise seasonally snow-free but have considerable vegetation (as evident in ASTER scenes, not shown), which produces low coherence in the image. Thus, high coherence occurs only in those areas recently exposed by glacial retreat and not yet covered by significant vegetation growth, i.e. only near the glacier snout.

See Table 3 for the snout positions obtained during the period of Pair 1 (2004–2005), Pair 5, and Pair 6 (2009–2010). These results correlate very well with the snout positions reported in a previous study, using ground-based surveys (Kumar et al. 2008). The colour code used in Figure 2(*a*) and (*b*) shows two dominant shades, blue representing low coherence, which is quite apparent over this region since continuous snowfall and melting, renders most of the region incoherent. The assumption made here is that the newly exposed surface material adjacent to the snout of the glacier, deposited by continuous recession of the terminus, should show coherence values well above 40% and is represented by red zones near the northern flank of the glacier in Figure 2(*a*) and (*b*). The average recession rate of the Gangotri glacier for the period 2004–2010, based on the distance between the two snout positions (along the central flow line of the glacier), obtained from the coherence maps (Table 3), is estimated to be 21.3 ± 3 m year^{-1}.

The recession trend is indirectly linked to the glacier mass balance, which is the net accumulation and ablation within a year measured as the difference between the amount of snow accumulated in winter and ice removed by melting in summer. The coherence maps computed from each of the pairs provide insight into the extent of ice-free surface observed during the respective time periods. Hence, stacking each of these coherence maps will highlight the area over which terminus retreat has occurred over the entire period of 2004–2010, yielding a holistic view of the ice-free area cleared by ice over the region covered by the Gangotri glacier and its tributaries. Figure 3 shows the colour-coded coherence map obtained by stacking the coherence images from Pairs 1, 5, and 6. This represents
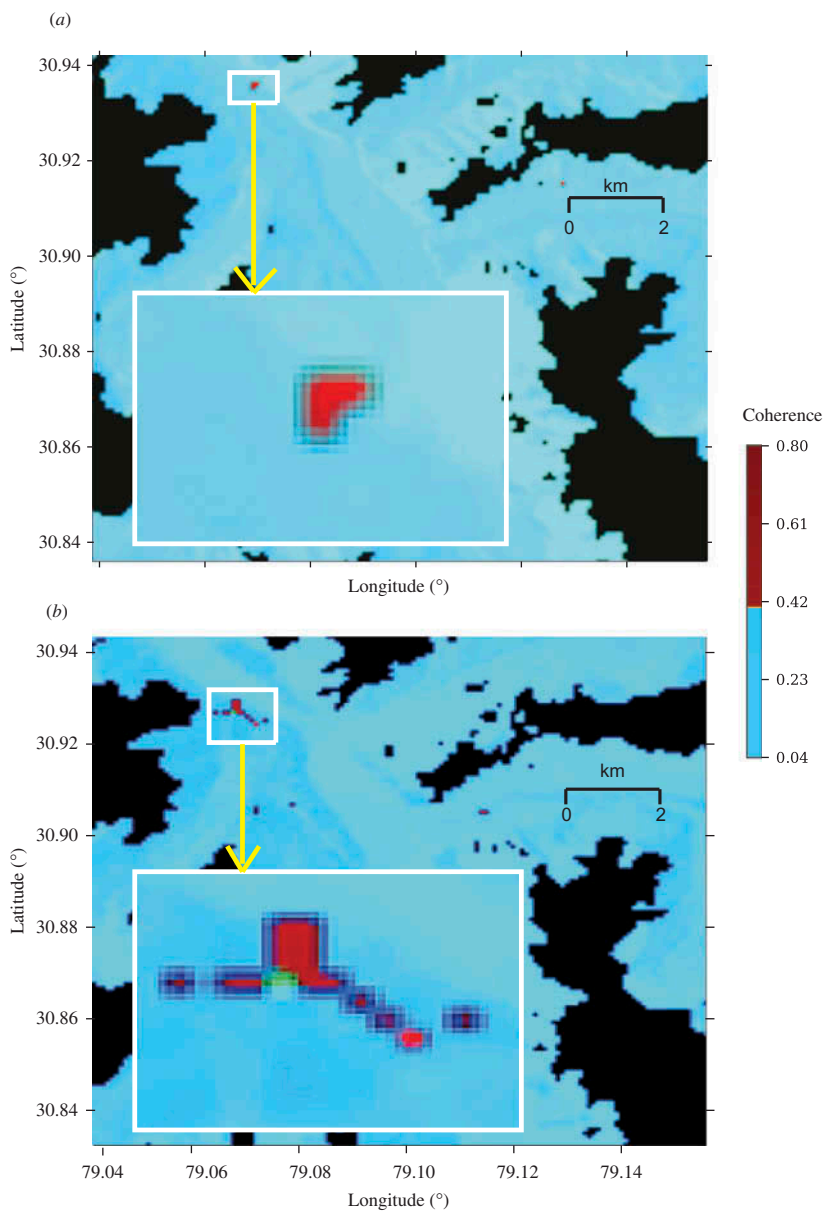
Figure 2. (*a*) Coherence map corresponding to the interferogram of Pair 1 (2004–2005) and (*b*) coherence map corresponding to the interferogram of Pair 6 (2009–2010). Illustrated are the highly coherent areas (shown as red zone in box) near the snout of the Gangotri glacier over the respective time periods. The colour scale shows degree of coherence, where red corresponds to a high degree (>40%) of coherency and blue to a low degree (<40%).

the region over which ice melted during 2004–2010 (interval between image Pair 1 and image Pair 6). High coherence values indicate areas that have been most stable during the entire period (2004–2010) and are inferred to be areas from which the glacier has receded permanently. Three prominent areas with very high coherence values, corresponding to

Table 3. Estimated snout positions from coherence maps obtained from each of the three pairs, given in decimal degrees.

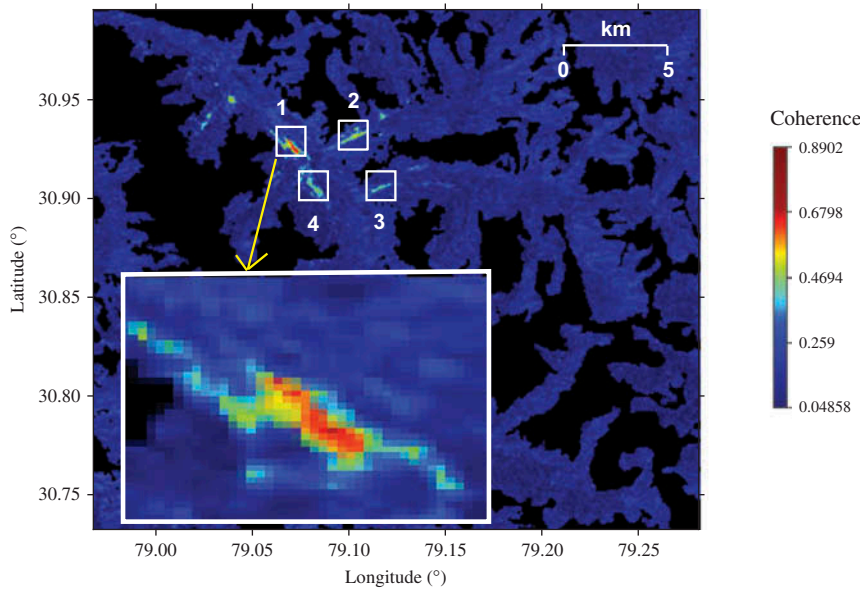| Pairs	Latitude	Longitude
Pair 1	30.9271 N	79.0794 W
Pair 5	30.9267 N	79.0792 W
Pair 6	30.9261 N	79.0791 W

Figure 3. Coherence image obtained from the stacking of coherence images obtained from each of the image pairs, 1, 5, and 6, representing changes measured between the periods of 2004 and 2010. Three prominent zones shown by boxes 1, 2, and 3 are the regions that were exposed due to melting during 2004–2010 near the snout of Gangotri, Raktvarna, and Chaturangi glaciers, respectively. Box 4 shows the downslope region of the Shivling Hills, which is the exposed ground, and not on the glacier. The main zone of interest (Box 1) is shown as an enlarged box marked by an arrow.

the snouts of Gangotri, Raktavarna, and Chaturangi glaciers, have been marked (1, 2, and 3, respectively) to show their total retreat during these years. The fourth region near the downslope of the Shivling Hills (refer to Figure 1) also shows good coherence, due to the fact that this is an ice-free region.

4.2. Glacier velocity measurements from 2005–2011

In this study, sub-pixel offset tracking analysis is performed on ASTER pairs, acquired around the month of October during 2005–2006, 2009–2010, and 2010–2011, that covered the entire Gangotri glacier in two frames. This enables a recent and periodic assessment of Gangotri glacier dynamics. Figure 4 represents a cumulative analysis plot of the Gangotri glacier motion. A Euclidean norm of the displacement measured in the north–south and east–west direction for Pair 2 and Pair 4 (2009–2010), after mosaicking, is shown in Figure 4(*a*). Large magnitudes of velocity are observed over the Gangotri glacier for both
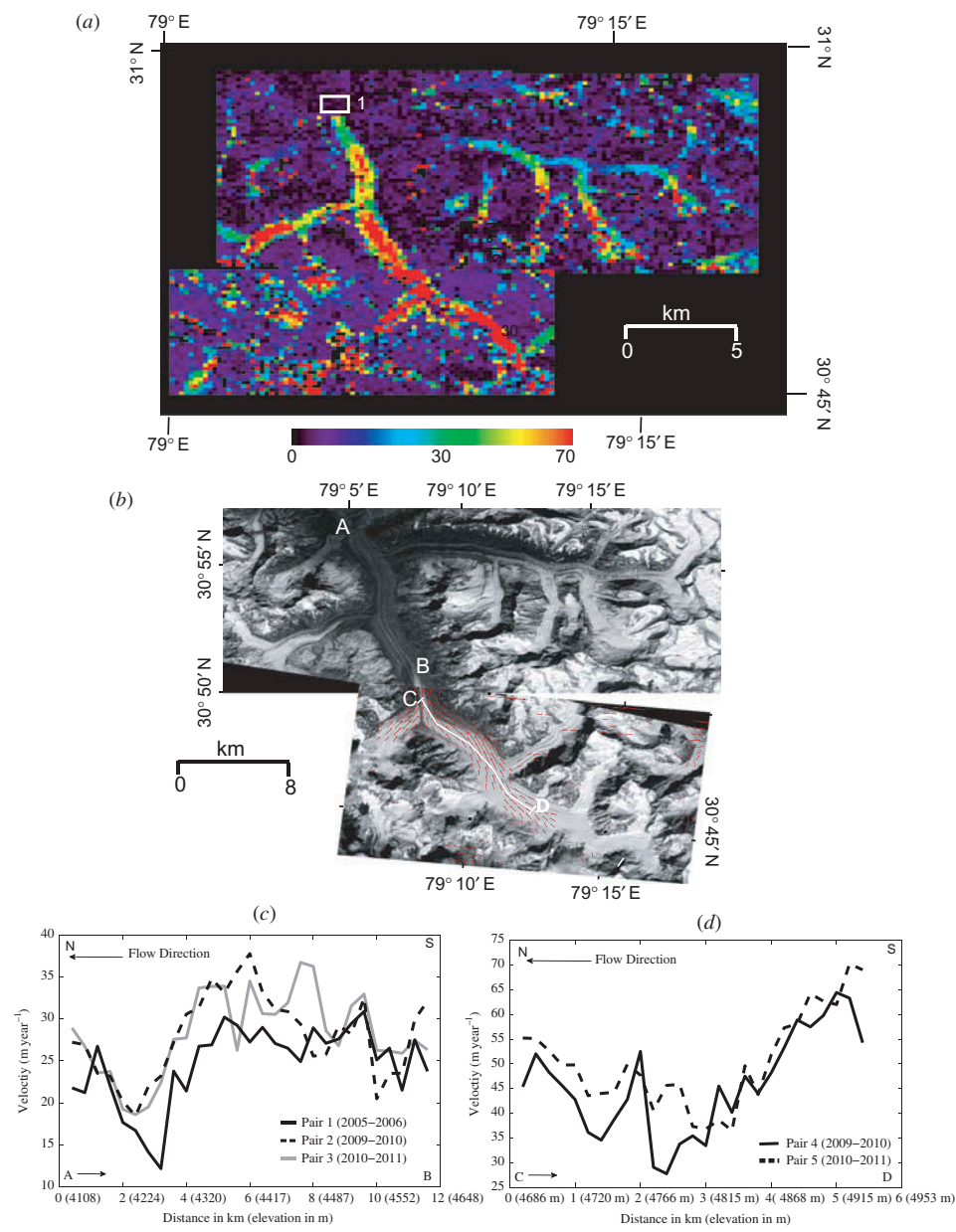
Figure 4. (*a*) Euclidean norm of the north–south and east–west displacement of the ASTER image Pair 1 and Pair 4 (mosaicked). The colour coding is applied to the pixels showing a displacement of 0–40 m and 0–70 m for Pair 1 and Pair 4, respectively, and higher values are discarded by filtering, Box 1 shows the ice-free region to calculate error in velocity estimates. (*b*) Vector field plot showing the flow trend of the Gangotri, the arrows indicate the direction of motion and the length of the arrow is proportional to the magnitude of the displacement. Arrows outside the glacier boundaries are the contributory noises arising from snow melting and the motion of the shadows casted by hills, (*c*) and (*d*) represent velocity *versus* distance along the profile lines (AB and CD) marked in (*b*) with elevation values, above mean sea level, along the profiles marked in braces.

pairs (indicated by bright red colour), with a maximum value of 40 ± 2.3 m year^{-1} in the lower glacier (Pair 1) and 70.2 ± 2.3 m year^{-1} in the upper glacier (Pair 4). Considering the time difference between the two concerned pairs, the velocity of the Gangotri glacier, during this period, is estimated to be a maximum of 70.2 m year^{-1} near the head of the glacier and less than 30 ± 2.3 m year^{-1} near the snout of the glacier. It is also evident from Figure 4(*a*) that the Gangotri glacier recorded higher motion than the surrounding region of steep mountain slopes, which had near zero net motion. A clear indication of glacier movement is also apparent from the definite pattern of motion illustrated in the vector field plot shown in Figure 4(*b*). Streamlines of velocity vectors (shown in Figure 4(*b*)) clearly demarcate the glacier extent and illustrate the magnitude and direction of glacier ice motion.

In order to demonstrate, in greater detail, velocity variations within the Gangotri glacier during the span of 2005–2011, glacier surface velocity along the central flow line of Gangotri (Figure 4(*b*)) is analysed for each of the images pairs (Table 2). Shown in Figures 4(*c*) and (*d*) is the velocity *versus* distance curve drawn along the profile line (Line AB for Pairs 1, 2, and 3 and CD for Pair 4 and 5 in Figure 4(*b*)). As observed from the profile plot for the lower reaches of Gangotri (Figure 4(*c*)), surface velocity variation is almost similar for all the three pairs. However, the annual flow rate for Pair 1 (2005–2006) is comparatively lower than that of Pair 2 (2009–2010) and Pair 3 (2010–2011), particularly near the snout and in the lower reaches of the glacier. In general, surface velocity is larger at higher reaches of the glacier as compared to those near the lower reaches and is likely dependent on variations in the glacier slope, width, and thickness. This pattern is also evident from the profile plot for higher reaches of the glacier (Figure 4(*d*) (also see supplementary Figure S1 at http://dx.doi.org/10.1080/01431161.2013.845923), where the glacier mass velocity is considerably higher near the head of the Gangotri glacier, for both the image pairs. While surface velocity near the snout, for all the time periods, varied between 24.8 ± 2.3 to 28.9 ± 2.3 m year^{-1}, velocities away from the snout varied between a minimum of 13.9 ± 2.3 m year^{-1} to a maximum of 70.2 ± 2.3 m year^{-1} (in the upper reaches of the glacier). The average velocity for the image pairs, 1, 2, and 3, are 28.1 ± 2.3, 27.9 ± 2.3, and 28.2 ± 2.3 m year^{-1}, respectively, which is considerably lower than the average velocities for Pair 4 and Pair 5, which are 45.7 ± 2.3 and 50.4 ± 2.3 m year^{-1}, respectively.

5. Discussion

Glacier surface velocity and retreat rate are two very important parameters that are used to characterize glacier dynamics. This study has produced reliable estimates of both of these parameters. The methodology involved the utilization of coherence mapping and image stacking to locate and monitor snout movement as well as quantify the zone of melting over a considerable time span. The observed snout positions between 2004 and 2010 are commensurate with those observed in earlier studies. Gangotri glacier retreat rate observed in this study is comparable to rates of 23 m year^{-1} (for 1985–2001) (Hasnain, Ahmad, and Kumar 2004; Cruz et al. 2007), 17.15 m year^{-1} (1971–2004) (Raina 2009), 23.2 m year^{-1} (for 1968–2001) (Bhambri, Bolch, and Chaujar 2011a, 2011b), and 19.9 m year^{-1} (for 1965–2006) (Bhambri, Bolch, and Chaujar 2012). The most recent estimate of glacier retreat using the differential global positioning system (DGPS) and satellite imagery was obtained to be 17.59 m year^{-1} for the period of 1976–2009 (Kumar, Areendran, and Rao 2009). Table 4 summarizes some of the most recently published retreat rates of the Gangotri glacier. The retreat rate measured in this study corroborates well with most of the long-term

Table 4. Gangotri glacier retreat rate as measured by various authors.

Reference	Period	Rate (m year^{-1})
Hasnain, Ahmad, and Kumar (2004)	1985–2001	23
Cruz et al. (2007)	1985–2001	23
Kumar et al. (2008)	1965–2006	19.9
Thayyen (2008)	1971–2004	27.12
Raina (2009)	1971–2004	17.15
WWF (2009)	1976–2009	17.59
Bhambri, Bolch, and Chaujar (2011)	1968–2001	23.2
Bhambri, Bolch, and Chaujar (2012)	1965–2006	19.9
This study	2004–2010	21.3

measurements, estimated over the past 70 years, which also establishes the efficacy of the methodology presented here. And perhaps most importantly, the results presented here indicate that the most recent retreat rate of the Gangotri glacier confirms a continuous retreat of the glacier with a consistent rate taking into consideration multidecadal measurements. The current study also addresses the phenomenon of temporal decorrelation and associated limitations of InSAR with longer time intervals for surface velocity measurements and DEM generation for this particular region of the Eastern Himalayas. Sub-pixel offset tracking, utilizing ASTER data, enabled high-resolution measurements of surface ice-mass velocity, which is particularly relevant in difficult mountainous terrains such as that of the present study area (e.g. Scherler, Leprince, and Strecker 2008). A comprehensive analysis of surface velocity of the Gangotri glacier is performed for the entire length, from snout to the head, of the glacier. In general, the observed surface velocity variations of the Gangotri glacier are comparatively similar for the entire range of image pairs (between 2005 and 2011) acquired for this study. However, the magnitude of glacier motion is typically low for the period 2005–2006, which was also reported in Raina (2009). While the majority of the incongruence amongst the spatial distribution of surface velocity is noted in the upper reaches of the glacier, velocities near the snout are almost similar over all time periods. The annual variations are high, which indicates fast motion of the Gangotri glacier, especially during the period 2009–2011. These estimates are considerably higher than the short-term estimates made by Kumar, Venkataraman, and Hogda (2011), Kumar et al. (2011), and yearly estimates by Scherler, Leprince, and Strecker (2008). Such high surface velocities may indicate that ice motion in this region is dominated by basal sliding in the ablation zone of this relatively steep glacier. The velocities estimated here are based on cumulative surface displacement experienced by the glacier over a period of 1 year. Hence, these velocity estimates do not reflect on its seasonal variation. The surface velocity variations are most comparable for Pairs 2 and 3. However, on average, surface velocity is observed to be lower during 2005–2006 compared to 2010–2011. These year-to-year variations can be attributed to factors such as variations in meteorological conditions (Singh et al. 2006) and the amount of basal sliding (Scherler, Leprince, and Strecker 2008) over the years. However, yearly differences in the amount of basal sliding due to the variation in melt water flux can be a contributory factor.

The current study has the potential to provide an integrated assessment of glacier flow dynamics, to complement previous and future studies in the area and to provide a key methodology to delineate glacial lake formation (Quincey et al. 2007; Bolch et al. 2011), which is of major concern in the Himalayan glaciers.

6. Conclusions

This study provides comprehensive characterization of the dynamics of the Gangotri glacier in terms of retreat rate and surface velocity estimates over a continuous period from 2004 to 2010. We employed SAR interferometry to quantify the snout retreat of the Gangotri glacier in the Himalayas, exploring its capabilities for an integrated assessment of the glacier. Results showed that the Gangotri glacier, which is one of the largest Himalayan glaciers, retreated about 119 m over a period of 6 years (2004–2010), at an average rate of 21.3 ± 3 m year^{-1}. In the context of previous studies, the rate has been almost the same for the last couple of decades. The results also demonstrated that retreat rate of the terminus was not uniform over the 6-year period. Further, stacking coherence images from different SAR pairs delineated the area cleared by ice from 2004 to 2010, facilitating a broader idea about melting of Gangotri and its tributary glaciers. Results from the sub-pixel offset tracking of ASTER images revealed significant motion along the length of the glacier and its tributaries compared to the surrounding region, meanwhile establishing a better picture of flow characteristics of the Gangotri glacier. High velocities were observed at the upper reaches of the glacier while comparatively less movement was observed near the snout. Specifically, while the average glacier surface velocity was estimated to be about 36.1 ± 2.3 m year^{-1}, over the period 2005–2011, the maximum and minimum velocities ranged between 13.9 ± 2.3 and 70.2 ± 2.3 m year^{-1}. Overall, variation of surface velocity of ice mass over the entire length of the Gangotri glacier was approximately similar for all of the image pairs studied for the period 2005–2011. While most previous studies suggest a decrease in retreat rate based on observations made over short time period (e.g. Kumar et al. 2008), our study, which is based on almost continuous measurements over a period of 6 years, suggests that the glacier is melting at a constant rate, which is in accordance with long-term estimates measured since 1965. Such observations are useful in assessing the glacier's response to climate change and provide an avenue to understand glacier dynamics and its relation to glacier surface morphology.

Supplemental data

Supplemental data for this article can be accessed at http://dx.doi.org/10.1080/01431161.2013.845923.

References

Ashraf, A., R. Naz, and R. Roohi. 2012. "Glacial Lake Outburst Flood Hazards in Hindukush, Karakoram and Himalayan Ranges of Pakistan: Implications and Risk Analysis." *Geomatic, Natural Hazards and Risk Analysis* 3: 113–132.

Atwood, D. K., F. Meyer, and A. Arendt. 2010. "Using L-Band SAR Coherence to Delineate Glacier Extent." *Canadian Journal of Remote Sensing* 36: 186–195.

Bagla, P. 2009. "No Sign yet of Himalayan Meltdown, Indian Report Finds." *Science* 326: 924–925.

Bajracharya, S. R., and B. R. Shrestha. 2011. *The Status of Glaciers in the Hindu Kush-Himalayan Region*. Kathmandu: ICIMOD.

Barnett, T. P., J. C. Adam, and D. P. Letternmaier. 2005. "Potential Impacts of a Warming Climate on Water Availability in Snow Dominated Regions." *Nature* 438: 303–309.

Bhambri, R., T. Bolch, and R. K. Chaujar. 2011a. "Mapping of Debris-Covered Glaciers in the Garhwal Himalayas Using ASTER DEMs and Thermal Data." *International Journal of Remote Sensing* 32: 8095–8119.

Bhambri, R., T. Bolch, and R. K. Chaujar. 2011b. "Glacier Changes in the Garhwal Himalaya, India, From 1968 to 2006 Based on Remote Sensing." *Journal of Glaciology* 57: 543–556.

Bhambri, R., T. Bolch, and R. K. Chaujar. 2012. "Frontal Recession of Gangotri Glacier, Garhwal Himalayas, From 1965 to 2006, Measured Through High-Resolution Remote Sensing Data." *Current Science* 102: 489–494.

Bindschadler, R. A., and T. A. Scambos. 1991. "Satellite-Image-Derived Velocity field of an Antarctic Ice Stream." *Science* 252: 242–252.

Bolch, T., A. Kulkarni, A. Kääb, C. Huggel, F. Paul, G. Cogley, H. Frey, J. S. Kargel, K. Fujita, M. Scheel, S. Bajracharya, and M. Stoffel. 2012. "The State and Fate of Himalayan Glaciers." *Science* 336: 310–314.

Bolch, T., J. Peters, B. Pradhan, A. B. Yegorov, M. F. Buchroithner, and V. P. Blagoveshchenskiy. 2011. "Identification of Potentially Dangerous Glacial Lakes in the Northern Tien Shan." *Natural Hazards* 59: 1691–1714.

Bolch, T., T. Pieczonka, and D. I. Benn. 2011. "Multi-Decadal Mass Loss of Glaciers in the Everest Area (Nepal Himalaya) Derived From Stereo Imagery." *The Cryosphere* 5: 349–358.

Capps, D. M., B. Rabus, J. J. Clague, and D. H. Shugar. 2010. "Identification and Characterization of Alpine Subglacial Lakes Using Interferometric Synthetic Aperture Radar (InSAR): Brady Glacier, Alaska, USA." *Journal of Glaciology* 56: 861–870.

Cogley, J. G., J. S. Kargel, G. Kaser, and C. J. Van der Veen. 2010. "Tracking the Source of Glacier Misinformation." *Science* 327: 522. doi:10.1126/science.327.5965.522-a.

Crippen, R. E. 1992. "Measurement of Subresolution Terrain Displacements Using SPOT Panchromatic Imagery." *Episodes* 15: 56–61.

Cruz, R. V., H. Harasawa, M. Lal, S. Wu, Y. Anokhin, B. Punsalmaa, Y. Honda, M. Jafari, C. Li, and N. Huu Ninh. 2007. "Asia, in Climate Change 2007: Impacts, Adaptation and Vulnerability." In *Contribution of Working Group II to the Fourth Assessment Report of the Intergovernmental Panel on Climate Change*, edited by M. Parry, O. Canziani, J. Palutikof, P. van der Linden, and C. Hansen, 469–506. Cambridge: Cambridge University Press.

Debella-Gilo, M., and A. Kääb. 2011. "Sub-Pixel Precision Image Matching for Measuring Surface Displacements on Mass Movements Using Normalized Cross-Correlation." *Remote Sensing of Environment* 115: 130–142.

Dobhal, D. P., J. T. Gergan, and R. J. Thayyen. 2008. "Mass Balance Studies of Dokriani Glacier from 1992 to 2000, Garhwal Himalaya, India." *Bulletin of Glaciological Research, Japanese Society of Snow and Ice* 25: 9–17.

Dyurgerov, M. B., and M. F. Meier. 2005. *Glaciers and the Changing Earth System: A 2004 Snapshot*. Occasional Paper, 58: 117, Boulder, CO: Institute of Arctic and Alpine Research. http://instaar. colorado.edu/other/occ_papers. html

Fielding, E. J., M. Talebian, P. A. Rosen, H. Nazari, J. A. Jackson, M. Ghorashi, and M. Berberian. 2005. "Surface Ruptures and Building Damage of the 2003 Bam, Iran Earthquake Mapped by Satellite Synthetic Aperture Radar Interferometric Correlation." *Journal of Geophysical Research* 110: B3, B03302. doi:10.1029/2004JB003299.

Frey, H., F. Paul, and T. Strozzi. 2012. "Compilation of a Glacier Inventory for the Western Himalayas from Satellite Data: Methods, Challenges, and Results." *Remote Sensing of Environment* 124: 832–843.

Govindha, R. K. B. 2010. "Remote Sensing Based Hazard Assessment of Glacial Lakes: A Case Study in Zanskar Basin, Jammu and Kashmir, India." *Geomatics, Natural Hazard and Risk* 1: 339–347.

Hasnain, S. I., S. Ahmad, and R. Kumar. 2004. "Impact of Climate Change on Chhota Shigri Glacier, Chenab Basin, Gangotri Glacier and Ganga Headwater in the Himalaya." In *Proceedings, NATCOM-V&A Workshop on Vulnerability Assessment and Adaptation due to Climate Change on Indian Water Resources*, *Coastal Zones and Human Health*, edited by A. K. Gosain,

S. K. Sharma, A. Garg, S. Bhattacharya, and S. Rao, IIT Delhi, June 27–28, 2003, 1–7. Delhi: Government of India, Ministry of Environment and Forest.

Herman, F., B. Anderson, and S. Leprince. 2011. "Mountain Glacier Velocity Variation During a Retreat/Advance Cycle Quantified Using Sub-Pixel Analysis of ASTER Images." *Journal of Glaciology* 57: 197–207.

Howat, I. M., I. Joughin, M. A. Fahnestock, B. E. Smith, and T. Scambos. 2008. "Synchronous Retreat and Acceleration of Southeast Greenland Outlet Glaciers 2000–06: Ice Dynamics and Coupling to Climate." *Journal of Glaciology* 54: 646–660.

Immerzeel, W. W., L. P. van Beek, and M. F. Bierkens. 2010. "Climate Change Will Affect the Asian Water Towers." *Science* 328: 1382–1385.

Jacob, T., J. Wahr, W. T. Pfeffer, and S. Swenson. 2012. "Recent Contributions of Glaciers and Ice Caps to Sea Level Rise." *Nature* 482: 514–518.

Jain, S. 2008. "Impact of Retreat of Gangotri Glacier on the Flow of Ganga River." *Current Science* 95: 1012–1014.

Jain, S. K., P. K. Agarwal, and V. P. Singh, 2007. *Hydrology and Water Resources of India*. Springer Publication, ISBN 978-1-4020-5180-7.

Joughin, I., T. Slawek, R. Bindschadler, and S. F. Price. 2002. "Changes in West Antarctic Ice Stream Velocities: Observation and Analysis." *Journal of Geophysical Research* 107 (B11): 2289. doi:10.1029/2001JB001029.

Kääb, A. 2002. "Monitoring High-Mountain Terrain Deformation from Repeated Air- and Spaceborne Optical Data: Examples Using Digital Aerial Imagery and ASTER Data." *ISPRS Journal of Photogrammetry & Remote Sensing* 57: 39–52.

Kääb, A. 2005. "Combination of SRTM3 and Repeat ASTER Data for Deriving Alpine Glacier Flow Velocities in the Bhutan Himalaya." *Remote Sensing of Environment* 94: 463–474.

Kaser, G., M. Grosshauser, and B. Marzeion. 2010. "Contribution Potential of Glaciers to Water Availability in Different Climate Regimes." *PNAS USA* 107: 20223–20227.

Konig, M., J. Winther, and E. Isaksson. 2001. "Measuring Snow and Glacier Ice Properties from Satellite." *Reviews of Geophysics* 39: 1–27.

Kulkarni, A. V., B. P. Rathore, S. Mahajan, and P. Mathur. 2005. "Alarming Retreat of Parbati Glacier, Beas Basin, Himachal Pradesh." *Current Science* 88: 1844–1850.

Kulkarni, A. V., B. P. Rathore, S. K. Singh, and I. M. Bahuguna. 2011. "Understanding Changes in the Himalayan Cryosphere Using Remote Sensing Techniques." *International Journal of Remote Sensing* 32: 601–615.

Kumar, K., R. K. Dumka, M. S. Miral, G. S. Satyal, and M. Pant. 2008. "Estimation of Retreat Rate of Gangotri Glacier Using Rapid Static and Kinematic GPS Survey." *Current Science* 94: 258–262.

Kumar, R., G. Areendran, and P. Rao. 2009. *Witnessing Change: Glaciers in the Indian Himalayas*. WWF India. http://awsassets.wwfindia.org/downloads/glacier_report.pdf

Kumar, R., R. D. Singh, and K. D. Sharma. 2005. "Water Resources of India." *Current Science* 89: 794–811.

Kumar, V., G. Venkataraman, and K. A. Hogda. 2011. "Glacier Surface Velocity Estimation Using SAR Interferometry Technique Applying Ascending and Descending Passes in Himalayas." *International Journal of Applied Earth Observations and Geoinformation* 13: 545–551.

Kumar, V., G. Venkataraman, L. Larsen, and K. A. Hogda. 2011. "SAR Interferometry and Offset Tracking Approaches for Glacier Movement Estimation in the Himalaya." In *Proceedings, IEEE International Geoscience and Remote Sensing Symposium (IGARSS 2011)*, Vancouver, BC, July 24–29, 3175–3178.

Leprince, S., S. Barbot, F. Ayoub, and J. P. Avouac. 2007. "Automatic and Precise Orthorectification, Coregistration, and Subpixel Correlation of Satellite Images, Application to Ground Deformation Measurements." *IEEE Transaction on Geoscience & Remote Sensing* 45: 1529–1558.

Luckman, A., D. J. Quincey, and S. Bevan. 2007. "The Potential of Satellite Radar Interferometry and Feature Tracking for Monitoring Flow Rates of Himalayan Glaciers." *Remote Sensing Environment* 111: 172–181.

Mall, R. K., A. Gupta, R. Singh, R. S. Singh, and L. S. Rathore. 2006. "Water Resources and Climate Change: An Indian Perspective." *Current Science* 90: 1610–1626.

Meier, M. F., M. B. Dyurgerov, U. K. Rick, S. O'Neel, W. T. Pfeffer, R. S. Andersson, S. P. Andersson, and A. F. Glazovsky. 2007. "Glaciers Dominate Eustatic Sea Level Rise in the 21st Century." *Science* 317: 1064–1067. doi:10.1126/science.1143906.

Nakawo, M., H. Yabuki, and A. Sakai. 1999. "Characteristics of Khumbu Glacier, Nepal Himalaya: Recent Changes in the Debris-Covered Area." *Annals of Glaciology* 28: 118–122.

Negi, H. S., N. K. Thakur, A. Ganju, and X. X. Snehmani. 2012. "Monitoring of Gangotri Glacier Using Remote Sensing and Ground Observations." *Journal of Earth System Science* 121: 855–866.

Quincey, D. J., S. D. Richardson, A. Luckman, R. M. Lucas, J. M. Reynolds, M. J. Hambrey, and N. F. Glasser. 2007. "Early Recognition of Glacial Lake Hazards in the Himalaya Using Remote Sensing Datasets." *Global and Planetary Change* 56: 137–152.

Raina, V. K. 2009. *Himalayan Glaciers*. *A State-Of-Art Review of Glacial Studies*, *Glacial Retreat and Climate Change*. Ministry of Environment and Forests, India. http://moef.nic.in/downloads/publicinformation/MoEF%20Discussion%20Paper%20him.pdf

Richardson, S. D., and J. M. Reynolds. 2000. "An Overviewof Glacial Hazards in the Himalayas." *Quaternary International* 65/66: 31–47.

Rignot, E., and R. H. Thomas. 2002. "Mass Balance of Polar Ice Sheets." *Science* 297 (5586): 1502–1506.

Rodriguez, E., C. S. Morris, and J. E. Belz. 2006. "A Global Assessment of the SRTM Performance." *Photogrammetric Engineering and Remote Sensing* 72: 249–260.

Rosen, P. A., S. Hensley, G. Peltzer, and M. Simons. 2004. "Updated Repeat Orbit Interferometry Package Released." *Eos, Transactions, American Geophysical Union* 85: 47.

Scherler, D., S. Leprince, and M. R. Strecker. 2008. "Glacier-Surface Velocities in Alpine Terrain From Optical Satellite Imagery: Accuracy Improvement and Quality Assessment." *Remote Sensing of Environment* 108: 3806–3819.

Shrestha, A. B., M. Eriksson, and P. Mool. 2010. "Glacial Lake Outburst Flood Risk Assessment of Sun Koshi Basin, Nepal." *Geomatics, Natural Hazards and Risk* 1: 157–169.

Singh, P., U. K. Haritashya, N. Kumar, and Y. Singh. 2006. "Hydrological Characteristics of the Gangotri Glacier, Central Himalayas, India." *Journal of Hydrology* 327: 55–67.

Stearns, L. A., G. S. Hamilton, and N. Reeh. 2005. "Multi-Decadal Record of Ice Dynamics on Daugaard Jensen Gletscher, East Greenland, From Satellite Imagery and Terrestrial Measurements." *Annals of Glaciology* 42: 53–58.

Syed, T. H., J. S. Famiglietti, V. Zlotnicki, and M. Rodell. 2007. "Contemporary Estimates of Arctic Freshwater Discharge from GRACE and Reanalysis." *Geophysical Research Letters* 34: L19404. doi:10.1029/2007GL031254.

Thayyen, R. J. 2008. "Lower Recession Rate of Gangotri Glacier during 1971–2004." *Current Science* 95: 9–10.

Thayyen, R. J., and J. T. Gergan. 2010. "Role of Glaciers in Watershed Hydrology: A Preliminary Study of a 'Himalayan Catchment'." *The Cryosphere* 4: 115–128.

Willis, M. J., A. K. Melkonian, M. E. Pritchard, and J. M. Ramage. 2012. "Ice Loss Rates at the Northern Patagonian Icefield Derived Using a Decade of Satellite Remote Sensing." *Remote Sensing of Environment* 117: 184–198. doi:10.1016/j.rse.2011.09.017.